AB *INITIO* KINETICS OF THE REACTIONS BETWEEN BH_4^- + OH•

NGHIÊN CỨU CƠ CHẾ VÀ ĐỘNG HỌC CỦA PHẢN ỨNG BH_4^- + OH• BẰNG PHƯƠNG PHÁP HÓA LƯỢNG TỬ

Trinh Le Huyen[1], Dinh Quy Huong[2], Pham Thi Thu Thao[3], Tran Thi Thanh Huyen[1], Pham Cam Nam[1]*

[1]*The University of Danang- University of Science and Technology, Danang, Vietnam*
[2]*Department of Chemistry, University of Education, Hue University, Hue, Vietnam*
[3]*Sky-Line School, Vietnam*

*Corresponding author: pcnam@dut.udn.vn

(Received: May 22, 2023; Revised: August 15, 2023; Accepted: August 23, 2023)

Abstract - Tetrahydroborate anion (BH_4^-) in T_d symmetry group is a well-known hydrogen carrier, involved in various reactions to produce hydrogen gas. In this work, we reassessed the mechanism and kinetics of reactions between BH_4^- + OH• by using the DFT study. All of the structures in this reaction are optimized using the M062X/6-311++G(d,p) method. The solvent effect on the reaction mechanism was also taken into account by using the solvation model density (SMD). Based on the potential energy surfaces, the rate constants were also estimated by using the transition state theory (TST). It was discovered that the BH_4^- efficiently captures the free radical OH• in the gas phase. In an aqueous solution at a pressure of P = 1 atm and temperature of T = 298.15 K, the title reaction is controlled by diffusion effects, with a rate constant of $k_D = 9.4 \times 10^9$ $M^{-1}s^{-1}$.

Key words - Tetrahydroborate anion (BH_4^-); mechanism; DFT calculations; TST; kinetics

Tóm tắt – Tetrahydroborate anion (BH_4^-) thuộc nhóm đối xứng T_d, được biết đến như là một chất mang hydro, nó tham gia vào các phản ứng khác nhau để sản xuất khí hydro. Trong nghiên cứu này, chúng tôi tiến hành đánh giá cơ chế phản ứng và động học của phản ứng giữa BH_4^- + OH• bằng phương pháp lý thuyết phiếm hàm mật độ DFT. Các cấu trúc trong phản ứng này đã được tối ưu hóa bằng phương pháp M062X/6-311++G(d,p). Ảnh hưởng của dung môi lên cơ chế phản ứng được đánh giá thông qua mô hình SMD. Dựa trên bề mặt thế năng, các hằng số tốc độ cũng được thiết lập trên cơ sở lý thuyết trạng thái chuyển tiếp (TST). Kết quả tính toán cho thấy, trong pha khí BH_4^- là chất bắt gốc tự do hiệu quả. Trong nước tại P = 1 atm và T = 298.15 K phản ứng trên được khống chế bởi quá trình khuếch tán với hằng số tốc độ $k_D = 9.4 \times 10^9$ $M^{-1}.s^{-1}$.

Từ khóa - Tetrahydroborate anion (BH_4^-); cơ chế; tính toán DFT; lý thuyết TST; Động học

1. Introduction

The BH_4^- (tetrahydroborate or borohydride) anion plays several important roles in chemistry due to its unique properties as a reducing agent and its potential applications in various chemical processes [1-3]. Specially, the BH_4^- anion has been extensively studied as a potential hydrogen storage material [4-5]. The reaction between BH_4^- and OH• is an interesting chemical process with potential applications in various fields, including chemistry, materials science, and energy storage. This reaction is of interest because both BH_4^- and OH• are reactive species that play important roles in different chemical processes. BH_4^- is a strong reducing agent, meaning it can donate electrons to other compounds, while OH• is a powerful oxidizing agent that can abstract electrons from other molecules [6]. In addition, the reaction of BH_4^- and OH• plays a role in catalysis [7], where BH_4^- can be used as a reducing agent. Furthermore, the presence of BH_4^- in water, including species like H^+, OH^-, H•, and OH•, as a part of chemical processes involved in degrading pollutants such as chlorinated hydrocarbons during environmental remediation [8].

Despite its importance, the mechanism of the BH_4^- and OH• reaction is not fully understood, and several questions remain unanswered. For instance, what are the reaction intermediates and transition states involved in this reaction? How does the reaction pathway change with different reaction conditions, such as temperature and pH? What is the effect of solvent on the reaction mechanism? Addressing these questions is critical for understanding the kinetics and thermodynamics of this reaction and for optimizing its application in energy storage, catalysis, and environmental remediation.

Theoretical calculations have become an indispensable tool for understanding the reaction mechanism of complex systems, providing insights into reaction intermediates and transition states that are challenging to access experimentally. In this paper, we employ density functional theory (DFT) and transition state theory (TST) analysis to investigate the reaction mechanism of BH_4^- and OH•. Our calculations reveal crucial insights into the mechanism of this reaction, including the reaction intermediates and transition states involved. We explore the effect of temperature, and solvent on the reaction pathway, providing a comprehensive understanding of the kinetics and thermodynamics of this reaction.

Overall, our theoretical investigation of the mechanism of the reaction between BH_4^- and OH• provides important insights into the fundamental chemistry of this reaction. Our results offer new insights into the reaction intermediates and transition states involved and provide a foundation for designing and optimizing energy storage systems, catalysts, and environmental remediation processes. Our findings also suggest future experimental studies that can be conducted to validate our theoretical predictions and improve our understanding of the reaction mechanism.

2. Computational methods

We utilized density functional theory (DFT) with Minnesota Functional M06-2X [9] and the 6-311+G(d,p) basis set to perform geometry optimization on the BH_4^- anion in the presence of the hydroxyl radical. To simulate the influence of an aqueous solution, we employed a solvation model density (SMD) method [10], which fully immersed the molecules within a continuum of water. It has been established through careful prior investigations [11] that the SMD approach adequately captures the behavior of radical reactions in aqueous solutions. To determine the nature of each identified stationary point, subsequent calculations were carried out to obtain harmonic vibrational frequencies at the same computational level.

The study also involved a kinetic analysis of overall free radical in both gas and physiological environments. The solvation model density (SMD) was applied to analyze the kinetic behavior of the compounds in polar (water) environment. To improve the accuracy of the calculations, different functionals were used for thermochemistry and kinetics, which were previously established and justified. The rate constant (k) was computed based on the transition state theory and 1M standard state at 298.15 K using Equation (1) [12-19]. The calculations were conducted using the Gaussian 09 software suite [20].

$$k = \sigma\kappa \frac{k_B T}{h} e^{\frac{-(\Delta G^{\neq})}{RT}} \quad (1)$$

Where as: σ the reaction symmetry number, [21; 22]; κ tunneling corrections which were calculated using Eckart barrier [23]; k_B the Boltzmann constant; h the Planck constant; $\Delta G^{\neq}$ Gibbs free energy of activation.

3. Results and Disscusions

3.1. Structural parameters and electronic properties of BH_4^- anion in the gas phase and water

Figure 1 presents the optimized structures of BH_4^- anion and its radical ion, and protonation form in both the gas phase and water, using the M062X/6-311++G(d,p) method. In the gas phase, the B-H distance is 1.235 Å, which is shortened by approximately 0.012 Å in water, while maintaining *Td* symmetry (Figures 1a, b).

Upon donating one electron, the BH_4 form transforms into the C_{2V} group. In this configuration, the B-H bond distances separate into 1.179 Å and 1.290 Å, with the ∠HBH angles measuring 47.04° and 129.78°, respectively. These values are consistent with a study by *L. Andrew et al*. [24], which also reported a C_{2V} ground state for BH_4 with two long B-H bond lengths of 1.182 Å and 1.289 Å, along with acute and obtuse angles of 46.7° and 130.1°, respectively. These results validate the efficacy of our computational optimization method for calculating BH_4 and related complex structures. Similarly, in the presence of water solvent, the shape of BH_4 remains unchanged (Figures 1c and 1d).

Next, we investigate the behavior of BH_4^- when it accepts an H^+ ion to become BH_5. The ease of H^+ capture by BH_4^- is expressed through a proton affinity value of -328.17 kcal/mol. Upon protonation, the structure of BH_5 undergoes rearrangement, transitioning from neutral T_d symmetry to C_s symmetry. The C_s symmetry represents the global minimum of the BH_3-H_2 type, featuring interfragment B–H distances of (1.429 Å and 1.426 Å), with an elongated H_2 bond length of 0.799 Å (Figure 1e; 1f).

The computed values for BH_5 can be compared to the published results by M. S. *Schuurman et al*. [25], where BH_5 in the C_s configuration was optimized using the CCSD(T)/cc-pCTZ method, resulting in B–H bond lengths of (1.429 Å, 1.414 Å) and an elongated H_2 bond length of 0.801 Å.

Unlike BH_4 and BH_4^- anion, as we predicted, it appears that BH_5 in the C_s symmetry does not exist in an aqueous environment, as its structures exhibit a negative frequency in the twisting vibration of the two free H atoms adjacent to the BH_3 plane. That could be raise open the question of whether BH_5 stable in the solution.

Based on our calculation, it appears that BH_5 in the C_s symmetry configuration is not stable in an aqueous environment, unlike BH_4 and BH_4^- anion. This conclusion is supported by the observation that the structures of BH_5 exhibit a negative frequency in the twisting vibration of the two free H atoms adjacent to the BH_3 plane. As a result, this raises a crucial question about the stability of BH_5 in a solution. To address this question comprehensively, further investigation is necessary, combining both theoretical and experimental studies. A more in-depth analysis is required to fully understand the behavior and characteristics of BH_5 in different solvent environments.

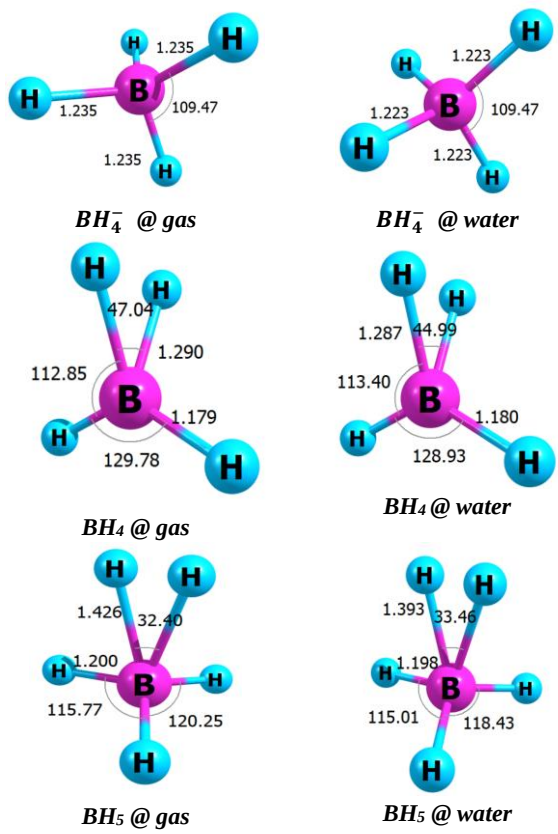

Figure 1. *Geometric shapes and some bond distances (angstrom) and bond angle (degree) in the gas phase and water solution of* ***a; b)*** *BH_4^- anion,* ***c; d)*** *BH_4 neutral,* ***e; f)*** *BH_5 neutral Optimized at UM062X/6-311++G(d,p) level*

3.2. FT-IR Spectrum of BH_4^- anion in the gas and water

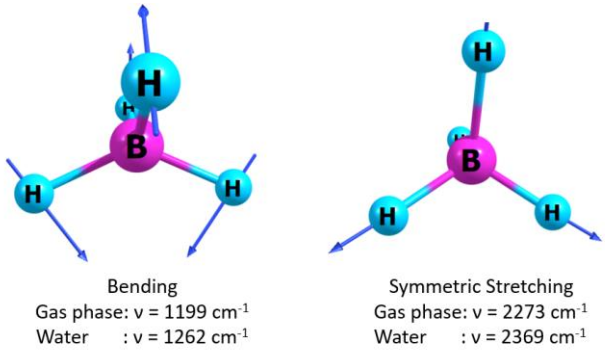

Figure 2. *The bending and stretching modes of BH_4^- anion in the gas phase and water were calculated using the M062X/6-311++G(d,p) theory level*

As mentioned previously, BH_4^- is a negatively charged anion consisting of boron and hydrogen atoms, arranged in a tetrahedral structure. The chemical bonding and molecular structure of BH_4^- can be examined using FT-IR (Fourier Transform Infrared) calculations, which detect the characteristic vibrations of its constituent atoms. In the infrared region of the electromagnetic spectrum, molecules absorb light energy corresponding to their vibrational transitions between different energy levels. Each type of chemical bond in BH_4^-, such as the B-H bonds, exhibits specific energy levels associated with their vibrations, resulting in distinctive absorption bands in the FT-IR spectrum. The FT-IR spectrum of BH_4^- typically exhibits several prominent peaks that correspond to various vibrational modes. Vibrational modes and their corresponding IR absorption bands for the BH_4^- anion have been plotted using M062X/6-311++G(d,p) (see Figure 2).

B-H Stretching: The stretching vibrations of the B-H bonds are observed at peaks of 2273 cm^{-1} and 2369 cm^{-1}, indicating the gas phase and water environments, respectively. These values align reasonably well with data obtained from *Ref [26]* in the 2000 ÷ 2500 cm^{-1} region. The precise peak location depends on the specific surroundings and coordination of the borohydride anion.

B-H Bending: The bending vibrations of the B-H bonds produce absorption bands at peaks of 1199 cm^{-1} and 1262 cm^{-1}, representing the gas phase and water environments, respectively. These values also agree well with *Ref* [26] in the 1000 ÷ 1500 cm^{-1} region. However, the exact positions of these peaks may vary depending on the molecular environment. Based on that, FT-IR spectroscopy can be utilized to investigate the interactions of BH_4^- with other compounds or surfaces. By monitoring changes in the FT-IR spectrum, we can explore binding sites, chemical reactions, and structural modifications involving BH_4^-.

3.3. Mechanism and kinetics of the reaction between BH_4^- + $OH^\bullet$ radical

3.3.1. Potential energy surfaces (PES) of the reactions $BH_4^- + OH^\bullet = BH_3^{\bullet-} + H_2O$ (2) in the gas phase

After establishing the dominance of the tetrameric BH_4^- anionic form in the gas phase, we investigate its reactivity in the reaction $BH_4^- + OH^\bullet \rightarrow BH_3^{\bullet-} + H_2O$ which is a water-forming reaction that occurs in a ring of 5 atoms of HO-H-BH. The optimized geometric parameters and relative energies of relevant stationary structures at the M062X/6-311++G(d,p) level are summarized in Figure 3.

The most stable form of the tetrahydroborate anion (T_d) is found to be involved as the starting point in this process. The reaction is initiated by its complexing with the hydroxyl radical ($OH^\bullet$) reactant, leading first to a pre-association complex LM1 (Figure 3a). However, this energetically stable complex is less stable on the free energy scale (ΔG^0 = 10.43 kcal/mol for the complex lying above the separated reactant BH_4^- + $OH^\bullet$ at 298.15 K, due to the large difference in entropy contributions).

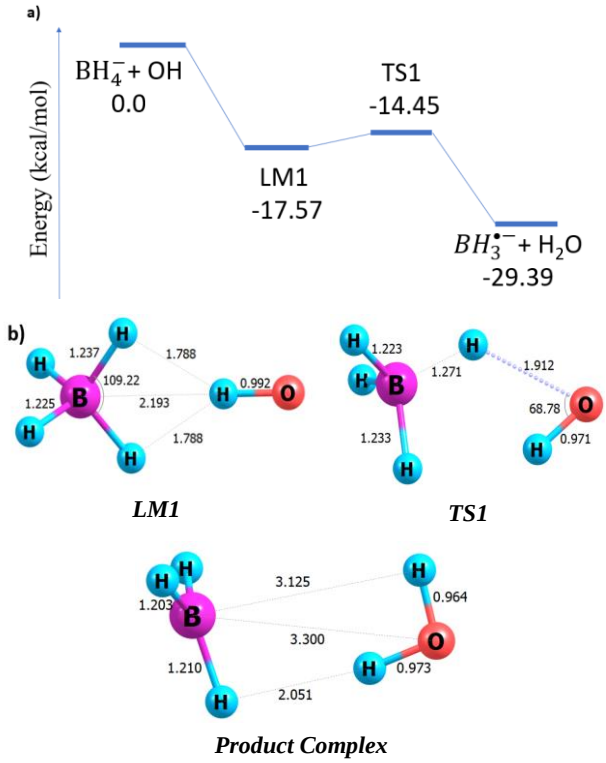

Figure 3. a) *Relative electronic energies (ΔE, values in kcal/mol, obtained from M062X/6-311++G(d,p) computations) of stationary points along the energy profile of BH_4^- + OH radical reaction in gas phase.* ***b)*** *Optimized geometries (M062X/6-311++G(d,p)), some bond distances (angstrom) and bond angle (degree)*

The transition structure **TS1** (Figure 3b) has negative energy barrier of 14.45 kcal/mol or higher than LM1 3.12 kcal/mol is characterized by successive hydrogen transfers giving another complex on the energy scale, which very easy splits apart to give a the $BH_3^{\bullet-}$ radical anion and H_2O molecule. The products lie below the reactants BH_4^- + $OH^\bullet$ (at 298K) by -29.39 kcal/mol.

In the transition structure TS1, the elimination of the H atom occurs within a range consisting of the HBH on the side closest to the free radical OH. As indicated by the imaginary vibrational mode of TS1, the H atom from BH_4^- anion is broken off to move to OH, while the OH radical also undergoes a rotational vibration, expanding the ∠HOH angle to 68.78 degrees to allow the O atom to easily capture the H atom from BH_4^-, forming H_2O. It is worth noting that the BH_4^- anion reactant in this reaction, which is a reducing

agent, uses its redundant electron to control the game by interacting with the OH radical.

3.3.2. Potential Energy Surfaces (PES) of the reactions $BH_4^- + OH^\bullet = BH_3^{\bullet-} + H_2O$ (2) in the water

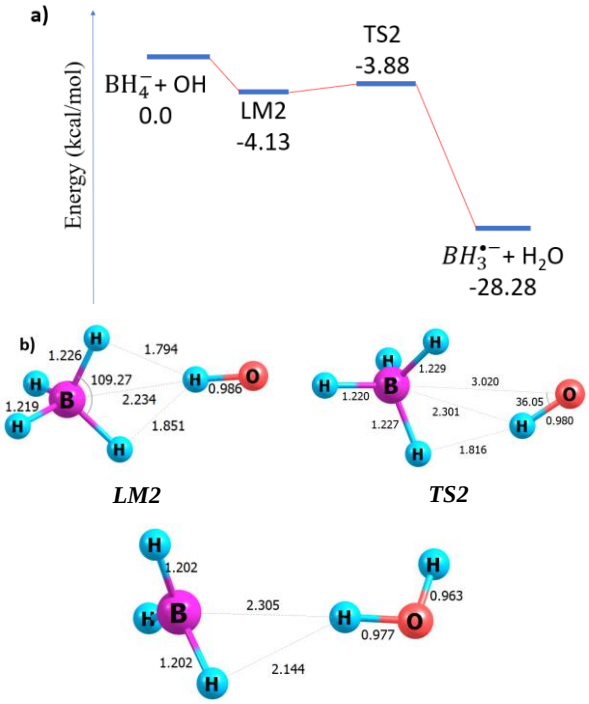

***Figure 4. a)** Relative electronic energies (ΔE, values in kcal/mol, obtained from UM062X/6-311++G(d,p) computations) of stationary points along the energy profile of BH_4^- + OH radical reaction in solution. **b)** Optimized geometries (UM062X/6-311++G(d,p)), some bond distances (angstrom) and bond angle (degree)*

Figure 4 shows a diagram of the potential energy profile that illustrates the reaction of BH_4^- with an $OH^\bullet$ radical in the solution, based on the energy calculations obtained using the UM062X/6-311++G(d,p) method in the combination with SMD model to simulate for solvent effect. Figure 4b presents the optimized geometric parameters of the reactants, intermediates, and product structures, which were also calculated using the same method. Additionally, the Cartesian coordinates of the main species involved in the BH_4^- + $OH^\bullet$ reaction, which were calculated and optimized at the UM062X/6-311++G(d,p) method.

The energies shown in Figure 4a were obtained using the UM062X/6-311++G(d,p) method. The initial combination of BH_4^- and $OH^\bullet$ proceeds through a pre-reaction complex named LM2 (shown in Figure 4a), which has a complexation energy of -4.13 kcal/mol less stable than LM1 (-17.57 kcal/mol) in the gas phase. This difference could be attributed to the distance between the molecules. In water, the (BH_4^---- $OH^\bullet$) bond is lengthened to 2.234 Å, compared to the value of 2.193 Å in the gas phase. LM2 is also formed in a similar shape to LM1, where the B-H bond in BH_4^- and OH lead to the formation of a new O-H bond, resulting in the creation of H_2O via TS2, which has a small positive energy barrier of 0.25 kcal/mol. The connections between TS2 and the two minimal complexes are confirmed by IRC calculations without ZPE.

The transition structure TS2 (shown in Figure 4b) is described as involving the splitting of BH_4^- through successive hydrogen transfers, resulting in the creation of another complex on the enthalpy scale. This complex then breaks apart to produce the $BH_3^{\bullet-}$ radical anion and H_2O. However, the product complex becomes less stable than the separated product on the free energy scale, due to a large entropic change (ΔG_0 = -26.16 kcal/mol for the product complex at 298.15 K, as shown in Figure S1). A closer examination of the imaginary vibrational mode of TS2 shows that the dissociation of the B-H bond occurs simultaneously with the rotation of the OH radical, leading to the formation of a H_2O molecule, which then associates with the $BH_3^{\bullet-}$ radical anion.

However, the energy barriers for this process are lower than those for the LM2 complex, with a value of 0.16 kcal/mol after correction for ZPE (as shown in Figure S2). This suggests that neither LM2 nor TS2 exist on the reaction pathway to control this reaction. The overall process in this reaction in water is exothermic, with a release of -28.28 kcal/mol, resulting in the production of H_2O and the $BH_3^{\bullet-}$ radical anion.

3.4. Kinetic study

The gas-phase reaction between BH_4^- and $OH^\bullet$, leading to the formation of $BH_3^{\bullet-}$ and H_2O, is undergoing the transition structure TS1, where direct hydrogen abstraction is expected to be the primary reaction pathway. The rates of this reaction can be evaluated using classical transition state theory (TST). The rate constants for the bimolecular reactions can be calculated based on the predicted geometric and energetic parameters of the structures depicted on the potential energy profile (Figure 3a). To determine these values, we utilized energies obtained from M062X/6-311++G(d,p) + ZPE computations, along with vibrational frequencies and rotational constants computed at the same level. The theoretical calculations, incorporating the predicted imaginary frequency of approximately 459i cm^{-1} for TS1, yield a rate constant of $k_1 = 3.07 \times 10^{18}$ M^{-1} s^{-1}. This high rate constant indicates that the reaction proceeds rapidly, demonstrating the efficient capture of the free radical $OH^\bullet$ by the BH_4^- anion in the gas phase. Furthermore, the influence of temperature on the reaction is explored within the range of 298.15 to 350 K (Table 1). In these temperature regimes, an increase in temperature can promote the formation of more stable intermediate species or products, thereby potentially impeding the overall reaction rate.

In the solution-phase reaction of $BH_4^- + OH^\bullet \rightarrow BH_3^{\bullet-} + H_2O$, our kinetic calculations indicate that the rate constant values, considering the diffusion of reactant molecules towards each other, is determined to be $k_D = 9.4 \times 10^9$ $M^{-1}.s^{-1}$ at 298.15 K. Table 2 displays the rate constants at different temperatures. Specifically, for the H-transfer process channel, a diffusion correction is applied, resulting in an apparent (k_{app}) rate constant of $k_{app} = 8.00 \times 10^9$ [$M^{-1}.s^{-1}$]. This correction accounts for the fact that the rate constant for diffusion (k_{TST}) significantly exceeds the rate constant for the reverse reaction (k_r) involving the conversion of the pre-complex (LM2) back into reactants.

Moreover, our findings reveal that TS2, which is the location of the reaction's occurrence, does not play a significant role due to very low energy barriers or the absence of such barriers. By employing quantum chemical computations and the results of kinetic calculations, we can now propose that the reaction rate of this process is effectively controlled by diffusion.

Table 1. *The rate constant in the gas phase of reaction (2)*

T(K)	k_{TST}($M^{-1}.s^{-1}$)	κ	k_1 ($M^{-1}.s^{-1}$)
298	k_{TST}($M^{-1}.s^{-1}$)	κ	k_1 ($M^{-1}.s^{-1}$)
300	2.53×10^{18}	1.2	3.07×10^{18}
310	2.17×10^{18}	1.2	2.71×10^{18}
320	1.08×10^{18}	1.2	1.32×10^{18}
330	5.84×10^{17}	1.2	7.23×10^{17}
340	3.19×10^{17}	1.2	3.79×10^{17}
350	1.81×10^{17}	1.2	2.17×10^{17}

Table 2. *The rate constant in the water of reaction (2)*

T(K)	k_2 ($M^{-1}.s^{-1}$)	k_D ($M^{-1}.s^{-1}$)	k_{app} ($M^{-1}.s^{-1}$)	κ
298	5.30×10^{10}	9.40×10^{9}	8.00×10^{9}	0.6
300	5.20×10^{10}	9.80×10^{9}	8.30×10^{9}	0.6
310	4.70×10^{10}	1.30×10^{10}	9.90×10^{9}	0.6
320	4.20×10^{10}	1.60×10^{10}	1.10×10^{10}	0.6
330	3.80×10^{10}	1.90×10^{10}	1.30×10^{10}	0.6
340	3.50×10^{10}	2.30×10^{10}	1.40×10^{10}	0.6
350	3.30×10^{10}	2.70×10^{10}	1.50×10^{10}	0.6

4. Conclusions

In the present theoretical study, we used electronic structure theory computations with density functional theory (M062X functional) in conjunction with large basis sets to optimize the geometries and calculate relative energies of the station point species of reaction (2) in the gas phase also in aqueous solution using the SMD method. The basic kinetics based on the transition state theory (TST) corrected including diffusion-limit were used for modeling the rate constants of reactions.

The structure of BH_4^- anions and its different ion forms has been examined in both gas and aqueous phases, and the calculated results along with FT-IR spectral analysis have shown consistent agreement with experimental data.

The reaction mechanism in the gas phase has been elucidated, and in conjunction with transition state theory, it reveals that the BH_4^- anion acts as a highly efficient scavenger for free radicals.

The reaction of $BH_4^- + OH^\bullet \rightarrow BH_3^{\bullet -} + H_2O$, in the aqueous solution at 1 atm ambient conditions provided by diffusion-control is a fast process characterized by a rate constant of k_D= 9.4×10^9 [$M^{-1}.s^{-1}$] and rate constant of $k_{app} = 8.00 \times 10^9$ [$M^{-1}.s^{-1}$].

Acknowledgments. This work was funded by University of Education, Hue University under a grant number T.23–TN–03.

REFERENCES

[1] J. Shi, Z. Ran, and F. Peng, "Promising four-coordinated organoboron emitters for organic light-emitting diodes", *Dyes and Pigments*, vol. 204, pp. 110383, 2022.

[2] Z. Huang, Su. Wang, R. D. Dewhurst, N. V. Ignat'ev, M. Finze, and H. Braunschweig, "Boron: Its Role in Energy-Related Processes and Applications", *Angew. Chem. Int. Ed.*, vol. 59, no. 23, pp. 8800–8816, 2020.

[3] C. W. Hamilton, R. T. Baker, A. Staubitz, and I. Manners, "B–N compounds for chemical hydrogenstorage", *Chem. Soc. Rev.*, vol. 38, no. 1, pp. 279–293, 2009.

[4] H. Hagemann, "Boron Hydrogen Compounds for Hydrogen Storage and as Solid Ionic Conductors", *Materials for Energy Conversion*, vol. 73, no. 11, pp. 868-873, 2019.

[5] H. Hagemann, "Boron Hydrogen Compounds: Hydrogen Storage and Battery Applications", *Molecules*, vol. 26, no. 24, pp. 7425, 2021.

[6] S. Marincean, M. Fritz, R. Scamp, and J. E. Jackson, "Mechanistic investigations in α-hydroxycarbonyls reduction by BH_4^-", *J. Phys. Org. Chem.*, vol. 25, no. 12, pp. 1186-1192, 2012.

[7] R. L. Yanus, G. Yardeni, E. Maimon, M. Saphier, I. Zilbermann, and D. Meyerstein, "BH_4^--Promoted, Radical-Initiated, Catalytic Oxidation of $(CH_3)_2SO$ by N_2O in Aqueous Solution", *Eur. J. Inorg. Chem*, vol. 2016, no. 8, pp. 1161-1164, 2016.

[8] J. Adhikary, M. Meistelman, A. Burg, D. Shamir, D. Meyerstein, and Y. Albo, "Reductive Dehalogenation of Monobromo- and Tribromoacetic Acid by Sodium Borohydride Catalyzed by Gold Nanoparticles Entrapped in Sol–Gel Matrices Follows Different Pathways", *Eur. J. Inorg. Chem.*, vol. 2017, no. 11, pp. 1510-1515, 2017.

[9] Y. Zhao and D. G. Truhlar, "The M06 suite of density functionals for main group thermochemistry, thermochemical kinetics, noncovalent interactions, excited states, and transition elements: two new functionals and systematic testing of four M06-class functionals and 12 other functionals", *Theor. Chem. Acc.*, vol. 120, pp. 215-241, 2008.

[10] A. V. Marenich, C. J. Cramer, and D. G. Truhlar, "Universal Solvation Model Based on Solute Electron Density and on a Continuum Model of the Solvent Defined by the Bulk Dielectric Constant and Atomic Surface Tensions", *J. Phys. Chem. B.*, vol. 113, no. 18, pp. 6378–6396, 2009.

[11] M. E. Anderson, B. Braïda, P. C. Hiberty, and T. R. Cundari, "Revealing a Decisive Role for Secondary Coordination Sphere Nucleophiles on Methane Activation", *J. Am. Chem. Soc.*, vol. 142, no. 6, pp. 3125–3131, 2020.

[12] E. Dzib, J. L. Cabellos, F. Ortíz-Chi, S. Pan, A. Galano, and G. Merino, "Eyringpy: A program for computing rate constants in the gas phase and in solution", *Int. J. Quantum Chem.*, vol. 119, no. 2, pp. e25686, 2019.

[13] M. G. Evans and M. Polanyi, "Some applications of the transition state method to the calculation of reaction velocities, especially in solution", *Trans. Faraday Soc.*, vol. 31, pp. 875-894, 1935.

[14] H. Eyring, "The Activated Complex in Chemical Reactions", *J. Chem. Phys.*, vol. 3, 1935, pp. 107-115.

[15] D. G. Truhlar, W. L. Hase, and J. T. Hynes, "Current status of transition-state theory", *J. Phys. Chem.*, vol. 87, no. 15, pp. 2664-2682, 1983.

[16] T. Furuncuoglu, I. Ugur, I. Degirmenci, and V. Aviyente, "Role of Chain Transfer Agents in Free Radical Polymerization Kinetics", *Macromolecules*, vol. 43, no. 4, pp. 1823-1835, 2010.

[17] E. Vélez *et al.*, "A computational study of stereospecifity in the thermal elimination reaction of menthyl benzoate in the gas phase", *J. Phys. Org. Chem.*, vol. 22, no. 10, pp. 971-977, 2009.

[18] E. Dzib, A. Quintal, F. Ortiz-Chi, G. Merino, "*Eyringpy 2.0*", Cinvestav, Merida, Yucatan 2021.

[19] H. Boulebd, A. Mechler, N. T. Hoa, and Q. V. Vo, "Thermodynamic and kinetic studies of the antiradical activity of 5-hydroxymethylfurfural: computational insights", *New. J. Chem.*, vol. 44, no. 23, pp. 9863-9869, 2020.

[20] M. J. Frisch, *et al*., *Gaussian 09. 2009*, Gaussian, Inc.: Wallingford, CT, USA.

[21] E. Pollak and P. Pechukas, "Symmetry numbers, not statistical factors, should be used in absolute rate theory and in Broensted relations", *J. Am. Chem. Soc.*, vol. 100, no. 10, pp. 2984-2991, 1978.

[22] A. Fernández-Ramos, B. A. Ellingson, R. Meana-Pañeda, J. M. Marques, and D. G. Truhlar, "Symmetry numbers and chemical reaction rates", *Theor. Chem. Acc.*, vol. 118, pp. 813-826, 2007.

[23] C. Eckart, "The Penetration of a Potential Barrier by Electrons", *Phy. Rev.*, vol. 35, no. 11, pp. 1303, 1930.

[24] L. Andrews and X. Wang, "Infrared Spectrum of the Novel Electron-Deficient BH_4 Radical in Solid Neon", *J. Am. Chem. Soc.*, vol. 124, no. 25, pp. 7280–7281, 2002.

[25] M. S. Schuurman, W. D. Allen, P. V. R. Schleyer, and H. F. Schaefer, "The highly anharmonic BH_5 potential energy surface characterized in the ab initio limit", *J. Chem. Phys.*, vol. 122, no. 10, pp. 104302, 2005.

[26] V. D'Anna, A. Spyratou, M. Sharma, and H. Hagemann, "FT-IR spectra of inorganic borohydrides", *Spectrochim. Acta A Mol. Biomol. Spectrosc.*, vol. 128, no. 15, pp. 902-906, 2014.

ELECTRONIC SUPPORTING INFORMATION (ESI)

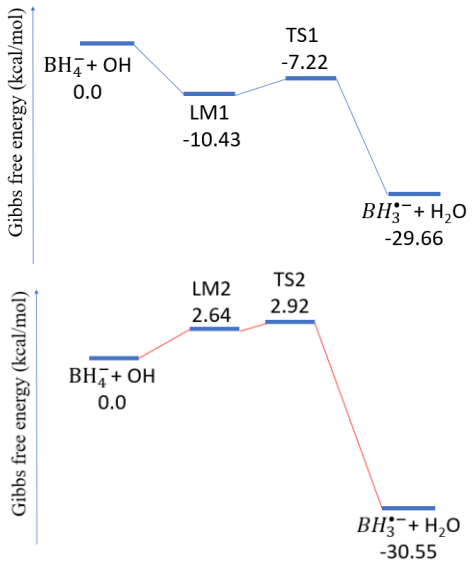

Figure S1. *Gibbs free energy of the reactions* $BH_4^- + OH^\bullet \rightarrow BH_3^- + H_2O$ (2) *in the gas phase (left) and in the water (right) computed at the M06-2X/6-311++G(d,p) level*

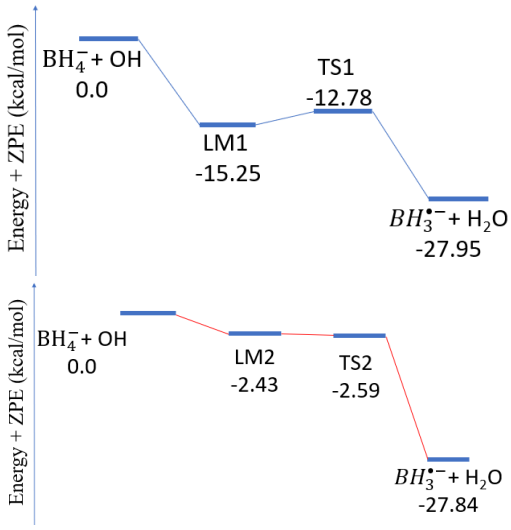

Figure S2. *Energy + ZPE of the reactions* $BH_4^- + OH^\bullet \rightarrow BH_3^- + H_2O$ (2) *in the gas phase (left) and in the water (right) computed at the M06-2X/6-311++G(d,p) levels*

Table S1. *Cartesian coordinates of all species were calculated at M06-2X/6-311++G(d,p) level of theory in the gas phase and solution*

BH_4^- @ gas phase

5	0.000000000	0.000000000	0.000000000
1	0.713033000	0.713033000	0.713033000
1	-0.713033000	0.713033000	-0.713033000
1	0.713033000	-0.713033000	-0.713033000
1	-0.713033000	-0.713033000	0.713033000

Zero-point correction= 0.033581 (Hartree/Particle)
Thermal correction to Energy= 0.036531
Thermal correction to Enthalpy= 0.037475
Thermal correction to Gibbs Free Energy= 0.015986
Sum of electronic and zero-point Energies= -27.201470
Sum of electronic and thermal Energies= -27.198520
Sum of electronic and thermal Enthalpies= -27.197576
Sum of electronic and thermal Free Energies= -27.219065

BH_4^- @ water

5	0.000000000	0.000000000	0.000000000
1	0.705854000	0.705854000	0.705854000
1	-0.705854000	-0.705854000	0.705854000
1	-0.705854000	0.705854000	-0.705854000
1	0.705854000	-0.705854000	-0.705854000

Zero-point correction= 0.035102 (Hartree/Particle)
Thermal correction to Energy= 0.038026
Thermal correction to Enthalpy= 0.038970
Thermal correction to Gibbs Free Energy= 0.017541
Sum of electronic and zero-point Energies= -27.303739
Sum of electronic and thermal Energies= -27.300815
Sum of electronic and thermal Enthalpies= -27.299870
Sum of electronic and thermal Free Energies= -27.321300

LM1

5	-1.540041000	0.000022000	-0.000004000
1	-0.823449000	0.002400000	1.008722000
1	-2.230265000	1.012399000	-0.003298000
1	-0.823476000	-0.004248000	-1.008740000
1	-2.232854000	-1.010578000	0.003332000
8	1.644699000	0.000019000	0.000001000
1	0.652658000	-0.000236000	0.000002000

Zero-point correction= 0.045867 (Hartree/Particle)
Thermal correction to Energy= 0.050961
Thermal correction to Enthalpy= 0.051906
Thermal correction to Gibbs Free Energy= 0.019037
Sum of electronic and zero-point Energies= -102.943764
Sum of electronic and thermal Energies= -102.938669
Sum of electronic and thermal Enthalpies= -102.937725
Sum of electronic and thermal Free Energies= -102.970594

TS1

5	1.401008000	0.008986000	0.000006000
1	0.343130000	0.714329000	0.000080000
1	2.018263000	0.286807000	1.018816000
1	1.072336000	-1.179700000	-0.000398000
1	2.018399000	0.287491000	-1.018531000
8	-1.455048000	0.064201000	0.000015000
1	-0.816789000	-0.667462000	-0.000121000

Zero-point correction= 0.044830 (Hartree/Particle)
Thermal correction to Energy= 0.049411
Thermal correction to Enthalpy= 0.050355
Thermal correction to Gibbs Free Energy= 0.019160
Sum of electronic and zero-point Energies= -102.939822
Sum of electronic and thermal Energies= -102.935242

Sum of electronic and thermal Enthalpies= -102.934297
Sum of electronic and thermal Free Energies= -102.965492

LM2

5	-1.555127000	0.000285000	0.002642000
1	-0.841463000	-0.051739000	0.997840000
1	-2.236884000	1.010311000	0.045699000
1	-0.849635000	0.032426000	-1.000120000
1	-2.263313000	-0.991464000	-0.037967000
8	1.661158000	0.000360000	0.005006000
1	0.677667000	-0.003837000	-0.058708000

Zero-point correction= 0.046292 (Hartree/Particle)
Thermal correction to Energy= 0.051581
Thermal correction to Enthalpy= 0.052525
Thermal correction to Gibbs Free Energy= 0.019894
Sum of electronic and zero-point Energies= -103.035115
Sum of electronic and thermal Energies= -103.029826
Sum of electronic and thermal Enthalpies= -103.028882
Sum of electronic and thermal Free Energies= -103.061513

TS2

5	-1.467947000	-0.016497000	0.002077000
1	-0.685365000	-0.868182000	-0.412634000
1	-1.698530000	-0.221927000	1.181923000
1	-0.957481000	1.092226000	-0.126248000
1	-2.496935000	-0.061492000	-0.650999000
8	1.551525000	-0.049233000	-0.000724000
1	0.765845000	0.535725000	0.003369000

Zero-point correction= 0.045651 (Hartree/Particle)
Thermal correction to Energy= 0.050407
Thermal correction to Enthalpy= 0.051351
Thermal correction to Gibbs Free Energy= 0.019941
Sum of electronic and zero-point Energies= -103.035368
Sum of electronic and thermal Energies= -103.030612
Sum of electronic and thermal Enthalpies= -103.029668
Sum of electronic and thermal Free Energies= -103.061078

$BH_3^{\bullet-}$ @ gas phase

5	0.000000000	0.000000000	0.000145000
1	0.000000000	1.205810000	-0.000241000
1	1.044262000	-0.602905000	-0.000241000
1	-1.044262000	-0.602905000	-0.000241000

Zero-point correction= 0.023699 (Hartree/Particle)
Thermal correction to Energy= 0.026758
Thermal correction to Enthalpy= 0.027702
Thermal correction to Gibbs Free Energy= 0.004742
Sum of electronic and zero-point Energies= -26.564736
Sum of electronic and thermal Energies= -26.561677
Sum of electronic and thermal Enthalpies= -26.560733
Sum of electronic and thermal Free Energies= -26.583693

$BH_3^{\bullet-}$ @ water

5	0.000647000	-0.000004000	0.000001000
1	1.201576000	-0.001921000	-0.000002000
1	-0.604078000	-1.037956000	-0.000002000
1	-0.600731000	1.039895000	-0.000002000

Zero-point correction= 0.022998 (Hartree/Particle)
Thermal correction to Energy= 0.026499
Thermal correction to Enthalpy= 0.027443
Thermal correction to Gibbs Free Energy= 0.002495
Sum of electronic and zero-point Energies= -26.662157
Sum of electronic and thermal Energies= -26.658656
Sum of electronic and thermal Enthalpies= -26.657712
Sum of electronic and thermal Free Energies= -26.682660

H_2O @ gas phase

1	0.761627000	-0.466527000	0.000000000
8	0.000000000	0.116614000	0.000000000
1	-0.761627000	-0.466387000	0.000000000

Zero-point correction= 0.021620 (Hartree/Particle)
Thermal correction to Energy= 0.024456
Thermal correction to Enthalpy= 0.025400
Thermal correction to Gibbs Free Energy= 0.003332
Sum of electronic and zero-point Energies= -76.399269
Sum of electronic and thermal Energies= -76.396433
Sum of electronic and thermal Enthalpies= -76.395489
Sum of electronic and thermal Free Energies= -76.417557

H_2O @ water

1	0.760235000	-0.472779000	0.000000000
8	0.000000000	0.118187000	0.000000000
1	-0.760235000	-0.472713000	0.000000000

Zero-point correction= 0.021293 (Hartree/Particle)
Thermal correction to Energy= 0.024130
Thermal correction to Enthalpy= 0.025074
Thermal correction to Gibbs Free Energy= 0.002991
Sum of electronic and zero-point Energies= -76.413449
Sum of electronic and thermal Energies= -76.410613
Sum of electronic and thermal Enthalpies= -76.409669
Sum of electronic and thermal Free Energies= -76.431752